Geophysical Research Letters

RESEARCH LETTER
10.1029/2020GL088996

Impacts of Shifting Subtropical Highs on the California Current and Canary Current Systems

Daniel F. Schmidt[1], Dillon J. Amaya[2], Kevin M. Grise[1], and Arthur J. Miller[3]

[1]Department of Environmental Sciences, University of Virginia, Charlottesville, VA, USA, [2]Oceans and Climate Lab, University of Colorado Boulder, Boulder, CO, USA, [3]CASPO Division, Scripps Institution of Oceanography, University of California, San Diego, La Jolla, CA, USA

Key Points:
- North Pacific subtropical high shifts explain much of the modeled trend in California Current system upwelling during boreal summer
- Shifts of the North Atlantic subtropical high have only modest impacts on the Canary Current system
- Both eastern boundary current systems are relatively insensitive to changes in the Northern Hemisphere Hadley cell

Supporting Information:
- Supporting Information S1

Correspondence to:
D. F. Schmidt,
dfs2uc@virginia.edu

Citation:
Schmidt, D. F., Amaya, D. J., Grise, K. M., & Miller, A. J. (2020). Impacts of shifting subtropical highs on the California Current and Canary Current systems. *Geophysical Research Letters*, *47*, e2020GL088996. https://doi.org/10.1029/2020GL088996

Received 26 MAY 2020
Accepted 7 JUL 2020
Accepted article online 17 JUL 2020

Abstract Upwelling in eastern boundary current regions is crucial to bringing nutrient-rich water to the photic zone and supporting the associated ecosystems. This upwelling is a result of the wind-driven ocean circulation and is therefore susceptible to changes in the atmospheric circulation. We use the Community Earth System Model and observational data to explore the response of upwelling in the California Current and Canary Current systems to shifts in the Northern Hemisphere subtropical high-pressure systems. We find that shifts in the North Pacific subtropical high explain a substantial fraction of both the short-term variability and projected trend in upwelling in the California Current system during boreal summer. By contrast, the Canary Current system is less affected by shifts of the North Atlantic subtropical high, mostly because the strongest wind anomalies associated with shifts of this high-pressure system occur too far north. We also find little impact from the Northern Hemisphere Hadley cell.

1. Introduction

Near-surface ocean currents are primarily wind driven. On the eastern sides of midlatitude oceans, for example, the eastern flanks of the subtropical high-pressure systems are associated with winds toward the equator which drive the eastern boundary currents. These currents in turn generate offshore movement of water by Ekman drift. In accordance with mass balance, this offshore movement is compensated by upwelling of deep, nutrient-rich water to the photic zone, which fuels some of the most productive marine ecosystems on Earth.

Anthropogenic climate change is expected to modify wind patterns in the future, and such changes could have major impacts on eastern boundary current ecosystems (Bakun et al., 2015; Jacox et al., 2016; Xiu et al., 2018). One possible source of such wind changes is the increase in land-sea temperature contrast with global warming (Bakun, 1990). This increased temperature gradient could amplify existing alongshore winds, thereby enhancing upwelling. However, attempts to detect this effect in observations or in climate models have yielded mixed results (Belmadani et al., 2014; Brady et al., 2017; Rykaczewski et al., 2015; Seo et al., 2012; Snyder et al., 2003; Sydeman et al., 2014; Wang et al., 2015).

In addition to this localized forcing, climate change can also drive shifts in larger-scale atmospheric circulation features, such as the subtropical highs or Hadley cells. The poleward expansion of the Hadley cells is a particularly well-studied example, and it is known to have impacts on surface-level climate (Amaya et al., 2018; Grise et al., 2019; Lu et al., 2007; Staten et al., 2018; Vallis et al., 2015). However, in boreal summer, the Northern Hemisphere (NH) Hadley cell is quite weak, and sinking air is split into very distinct high-pressure systems—the North Atlantic and North Pacific subtropical highs (NASH and NPSH, respectively). Furthermore, the descent in these high-pressure systems during summer is largely driven by monsoon heating over land, rather than by the zonal-mean meridional overturning circulation (i.e., the Hadley cell; Liu et al., 2004; Nigam & Chan, 2009; Rodwell & Hoskins, 2001). Like the Hadley cells, these subtropical highs can also shift due to climate change (He et al., 2017; Levine & Boos, 2019; Li, Li, & Kushnir, 2012; Li, Li, Ting, et al., 2012), and it is these shifts that are the more relevant processes for understanding changes to NH summer climate (Schmidt & Grise, 2019).

While the Bakun hypothesis for localized forcing of eastern boundary currents has generated considerable interest, few studies have investigated the impact of changes in larger-scale atmospheric circulation features, such as the subtropical highs, on eastern boundary current systems (with the exception of Rykaczewski

et al., 2015). In order to fill this gap, we will address the following two questions in this study: (1) How does upwelling respond to *short-term* (month-to-month) variability in the NH subtropical highs (i.e., the NASH and NPSH)? (2) How sensitive are modeled *long-term* (21st century) trends in upwelling to the future evolution of the NH subtropical highs? We will also briefly compare these results with the analogous results for the NH Hadley cell. We focus on the June-July-August (JJA) season, which roughly corresponds to the timing of peak chlorophyll in the two eastern boundary current regions of the NH (the California Current and Canary Current systems).

We find that variability in the position and strength of the NPSH does in fact explain a significant portion of the short-term variability in upwelling in the California Current region. Furthermore, using a large ensemble of simulations from the Community Earth System Model (CESM), we find that much of the uncertainty in 21st century upwelling trends across model ensemble members can also be attributed to uncertainty in the future evolution of the NPSH. The Canary Current system, however, is less sensitive to variability and 21st century trends in the position and strength of the NASH.

2. Data and Methods

2.1. Data

In this study, we use a combination of model output, observations, and reanalysis products. To study short-term variability, we use monthly mean output from the first 500 years of a 1,800 year fully coupled control run of the CESM (Kay et al., 2015; NCAR, 2015). In particular, we use sea level pressure (SLP) to calculate the positions and strengths of the subtropical highs, and upper-level meridional winds to calculate the width and strength of the NH Hadley cell. To study variability in upwelling and the simulated marine ecological response, we use the surface wind stress, surface ocean currents, upwelling at 50–60 m depth, and total chlorophyll averaged over depths of 0–100 m. Note that the results are not sensitive to the depth at which upwelling is examined. Chlorophyll is an indicator of nutrient availability driven by upwelling in the upper ocean, and the 0–100 m layer should be sufficient to include the entire photic zone and therefore essentially all chlorophyll.

To study 21st century trends, we use some of the same variables from the CESM Large Ensemble (CESM-LENS), which contains 40 runs of the same model under identical forcings—the Representative Concentration Pathway (RCP) 8.5 scenario from 2006 to 2100—but with differing initial conditions to represent the effects of unforced internal variability. We note that, due to the difficulties of modeling long-term trends in marine chlorophyll and net primary productivity (Rykaczewski & Dunne, 2010; Taucher & Oschlies, 2011), the winds should probably be regarded as the more reliable component of our trend analysis. Nonetheless, as we will show below, the wind and chlorophyll results are consistent with each other.

When possible, we validate the model-derived results by comparison with data from the European Centre for Medium-Range Weather Forecasts (ECMWF) Interim reanalysis data set (ERA-Interim; Dee et al., 2011; ECMWF, 2009). One slight difference between model and reanalysis variables is that—due to data availability—we use 10 m wind from ERA-Interim and surface wind stress from CESM. We also compare modeled chlorophyll with observations from the Sea-viewing Wide Field-of-view Sensor (SeaWiFS) on board the SeaStar satellite. We use monthly SeaWiFS data from January 1998 to December 2010, with a spatial resolution of 9.2 km (NASA Goddard, 2018; O'Reilly et al., 1998).

2.2. Methods

We compute the positions of the subtropical highs following the method described in Schmidt and Grise (2019). Briefly, we define the center of the NPSH in a given month as the centroid of the SLP > 1,018 hPa region within the rectangle 100–180°W, 0–60°N, and the center of the NASH as the centroid of the SLP > 1,018 hPa region within the rectangle 0–100°W, 0–60°N. Next, we define the strength of each high as the average SLP over a 10° longitude-by-10° latitude box centered at the location defined above (see also Song et al., 2018). We note that while these longitude, latitude, and strength indices are not completely independent, their correlations are small enough that all three are needed to characterize the state of each high-pressure system (see supporting information Table S1).

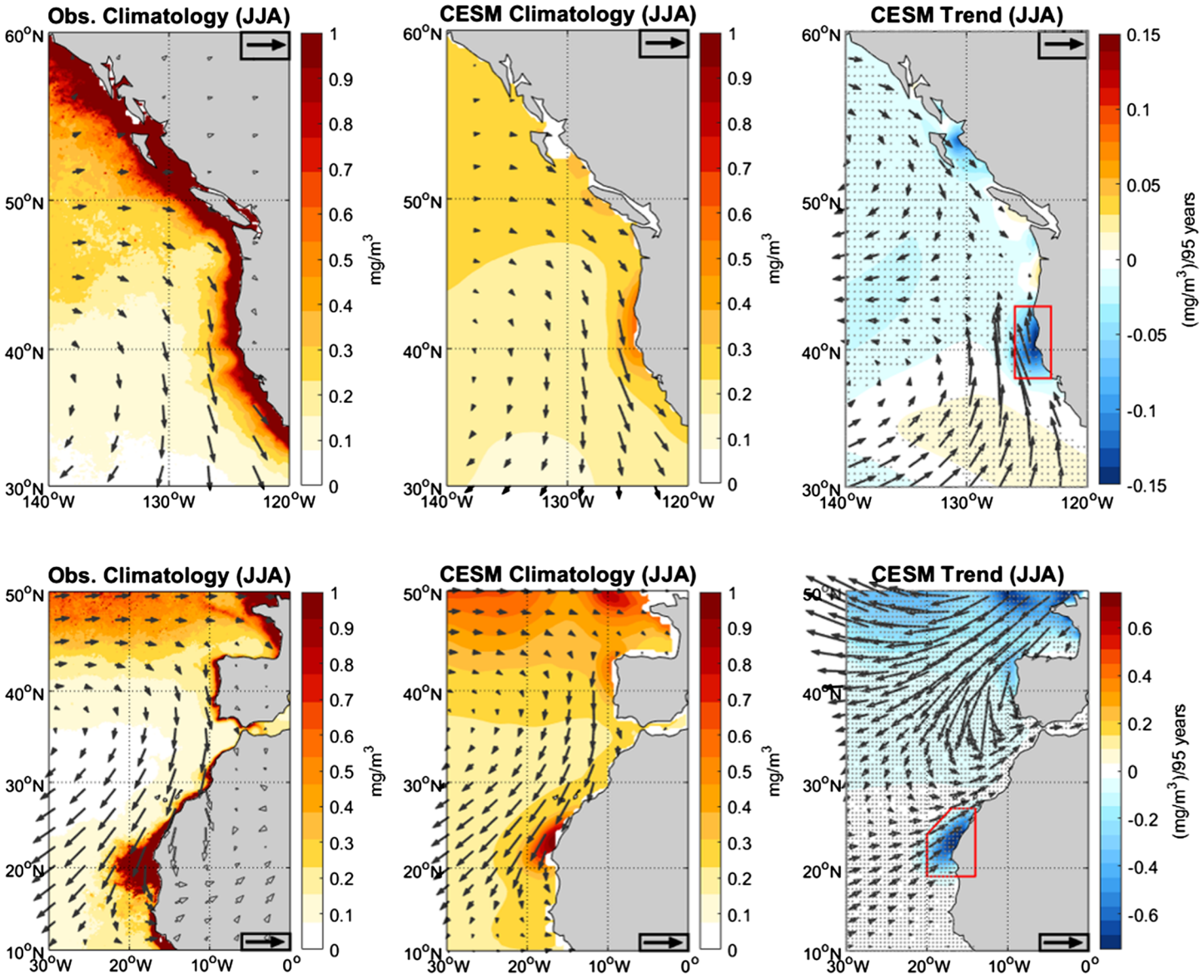

Figure 1. (left) Mean chlorophyll (colors) and wind (arrows) in the regions of the California Current and Canary Current, according to SeaWiFS satellite observations for the Period 1998–2010, and 10 m mean wind for the same period, using ERA-Interim data. The bold arrow in the corner represents a wind speed of 10 m/s, for scale. (center) Mean chlorophyll and wind stress according to the CESM coupled control run. The bold arrow represents a wind stress of 0.2 N/m^2. (right) Trends in total chlorophyll and surface wind stress, for the 2006–2100 RCP 8.5 portion of the CESM large ensemble, averaged over the 40 ensemble members. The bold arrow represents a wind stress trend of 0.02 N/m^2 per 95 years. Stippling indicates agreement of at least 80% of ensemble members on the sign of the trend. Note that the top right and bottom right panels have different color scales.

Four variables are relevant to understanding upwelling in eastern boundary currents: (1) surface wind stress, (2) surface current, (3) upwelling, and (4) chlorophyll. One can think of these as a causal chain, with each variable partly controlling the one that follows. We focus on surface wind stress and chlorophyll mostly because they represent the beginning and end of this chain. Nonetheless, it is worthwhile to verify that each of the four variables in this list is in fact correlated with the one that follows.

The correlations between alongshore wind stress and cross-shore surface current, or between cross-shore surface current and upwelling, are quite strong—in the range $0.72 \leq |r| \leq 0.94$—and of the expected sign (Figure S1). In contrast, the correlation between upwelling and chlorophyll in the California Current region is weak ($r = 0.09$), but this increases to $r = 0.40$ if chlorophyll is lagged by 1 month (i.e., June and July

upwelling correlated with July and August chlorophyll, with all values deseasonalized). For the Canary Current region, the correlation is strongest with no lag, at $r = 0.18$. Possible reasons for this delayed response in the California Current region include a deeper maximum nutrient concentration and slower average upwelling compared to the Canary Current, which would cause slower nutrient delivery to the surface—and slower responses to wind changes—in the former. Indeed, the profiles of dissolved inorganic nitrate, phosphate, and iron from the CESM control run all have peak concentrations at deeper levels in the California Current region, and upwelling is faster in the Canary Current region (not shown). Hence, in what follows, we apply a 1 month lag to chlorophyll for the California Current region. Without this lag, we would find similar conclusions, but the chlorophyll regressions and congruent trends would be somewhat weaker.

We will briefly consider whether the wind and chlorophyll changes associated with the subtropical highs could also be explained in terms of the simpler zonal-mean Hadley cell. We use a standard definition of the Hadley cell edge as the latitude at which the 500 hPa zonal-mean meridional mass stream function (Ψ_{500}) crosses 0 between 15°N and 45°N (see Solomon et al., 2016; Waugh et al., 2018). The strength of the Hadley cell is the maximum value of Ψ_{500} between the equator and the edge defined above. During the JJA season, the positions and strengths of the subtropical highs as defined above are poorly correlated with the strength and edge latitude of the NH Hadley cell (Schmidt & Grise, 2019), so the two may be treated to a reasonable approximation as separate processes.

3. Results

We begin by reviewing the observed and modeled climatology of the NH eastern boundary current regions. The top row of Figure 1 shows the JJA season climatological surface winds and chlorophyll in the California Current region according to observations (top left) and the CESM control run (top center). In both observations and CESM, the JJA climatology is characterized by northerly surface winds paralleling the coast of California along the eastern flank of the NPSH, with enhanced regions of chlorophyll along the North American Pacific coast and in the interior North Pacific Ocean. The modeled chlorophyll follows a similar spatial pattern to the observations but does not capture the magnitude or meridional extent of the sharp peak immediately off the coast—a point we will revisit later.

The bottom row of Figure 1 shows the analogous results for the Canary Current region. The observed climatology shows northerly surface winds off the Iberian Peninsula and northeasterly surface winds paralleling the African coast along the eastern flank of the NASH. The chlorophyll maximum is positioned off the African coast. The CESM climatology is similar, with the magnitude and meridional extent of the chlorophyll maximum underestimated (as in the California Current system).

The right column of Figure 1 shows the CESM simulated trends in chlorophyll and wind stress over the Period 2006–2100 under the RCP 8.5 scenario. Consistent with Figure 3 of Rykaczewski et al. (2015), a decrease in upwelling-favorable wind is apparent in the high-chlorophyll regions just off the coast. This is in contrast to the aforementioned Bakun hypothesis (Bakun, 1990), which would suggest an increase in upwelling-favorable winds in the same regions. So, if the Bakun hypothesis is operating, it is not strong enough to dominate the modeled trend. Instead, below, we investigate the role of the large-scale atmospheric circulation in driving the trends shown in the right column of Figure 1, focusing on the role of the subtropical highs.

3.1. Short-Term Variability

To understand better the role of the subtropical highs in driving changes in chlorophyll and wind stress, we first examine the relationship between short-term (month-to-month) variability in chlorophyll and wind stress with the subtropical highs. To do this, we compute the regressions of modeled surface wind stress and chlorophyll to the position and strength of the NPSH (Figure 2, top row) and NASH (Figure 2, bottom row) in the CESM control run. The corresponding correlations are in Table S2.

Figure 2 shows that an eastward shift of the NPSH (top left panel) is associated with southerly (upwelling-unfavorable) wind anomalies and, accordingly, negative chlorophyll anomalies. By contrast, both northward displacement and strengthening of the NPSH (top center and top right panels) are associated with northerly (upwelling-favorable) wind anomalies and corresponding positive anomalies in total chlorophyll. Note that

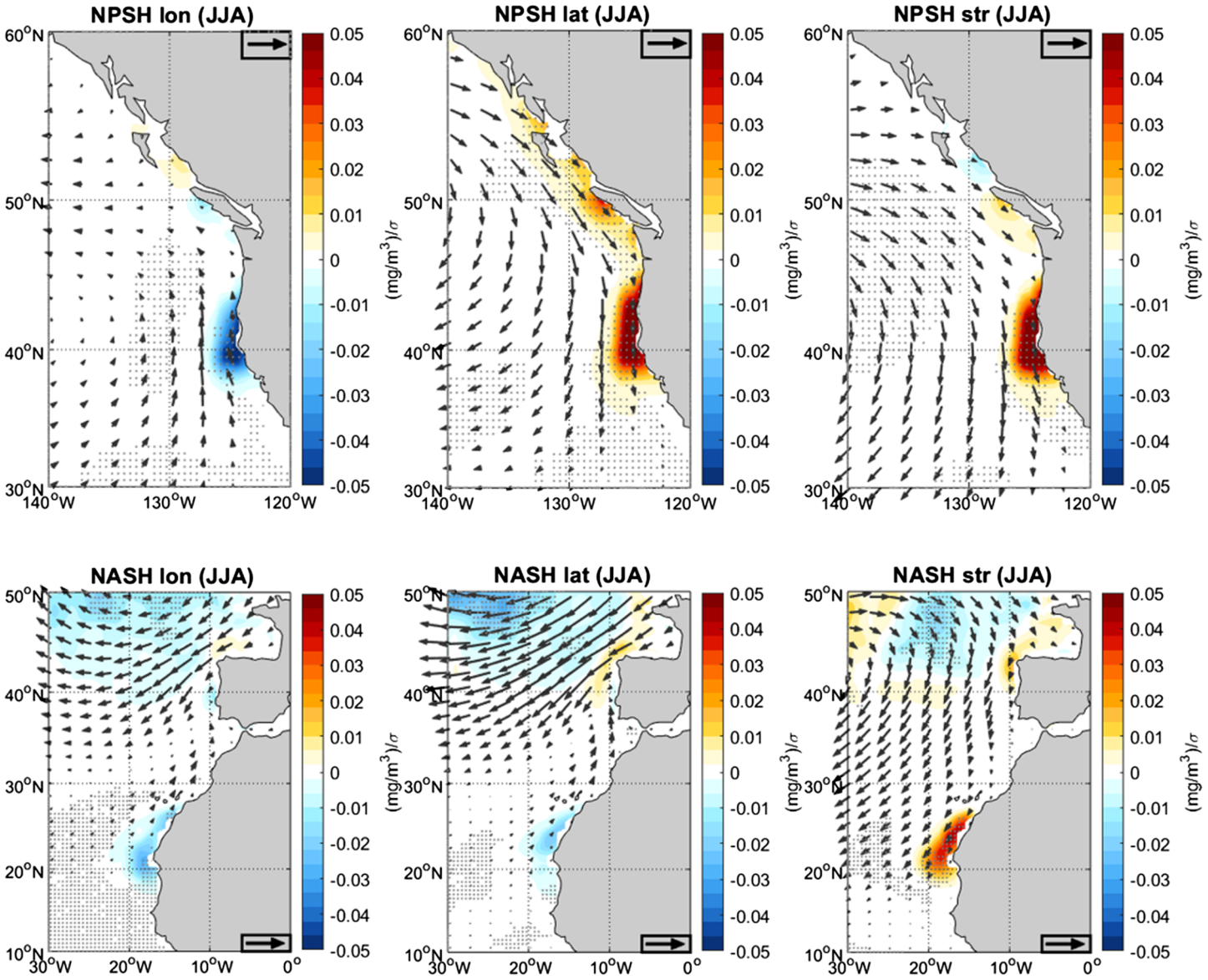

Figure 2. Regression of surface wind stress (arrows) and total chlorophyll (colors) to the NPSH indices (top row) and NASH indices (bottom row). All data are deseasonalized monthly means from the JJA seasons of the first 500 years of the CESM coupled control run. Sigma (σ) represents the standard deviation of the index. The bold arrow in the corner represents a wind stress regression of 0.02 (N/m^2)/sigma, for scale. Stippling indicates statistical significance of the chlorophyll regression at the $p < 0.05$ level. In the Pacific, chlorophyll is lagged by 1 month, whereas in the Atlantic, there is no lag, in accordance with the differing response times of chlorophyll in these two regions.

despite the similarity of these last two patterns, the NPSH latitude and strength are only weakly correlated ($r = 0.14$; Table S1).

By contrast, month-to-month variability in the NASH longitude and latitude does not have a significant impact on the upwelling in the Canary Current system along the African coast (Figure 2, bottom row). While shifts of the NASH position are associated with large wind anomalies, these mostly occur too far north to strongly affect the Canary Current. (Note that the Canary Current system is located at lower latitude than the California Current system, with a CESM chlorophyll maximum centered around 20–30°N for the former and 35–45°N for the latter). However, strengthening of the NASH does result in relatively strong northeasterly wind stress anomalies much closer to the African coast and corresponding positive chlorophyll anomalies.

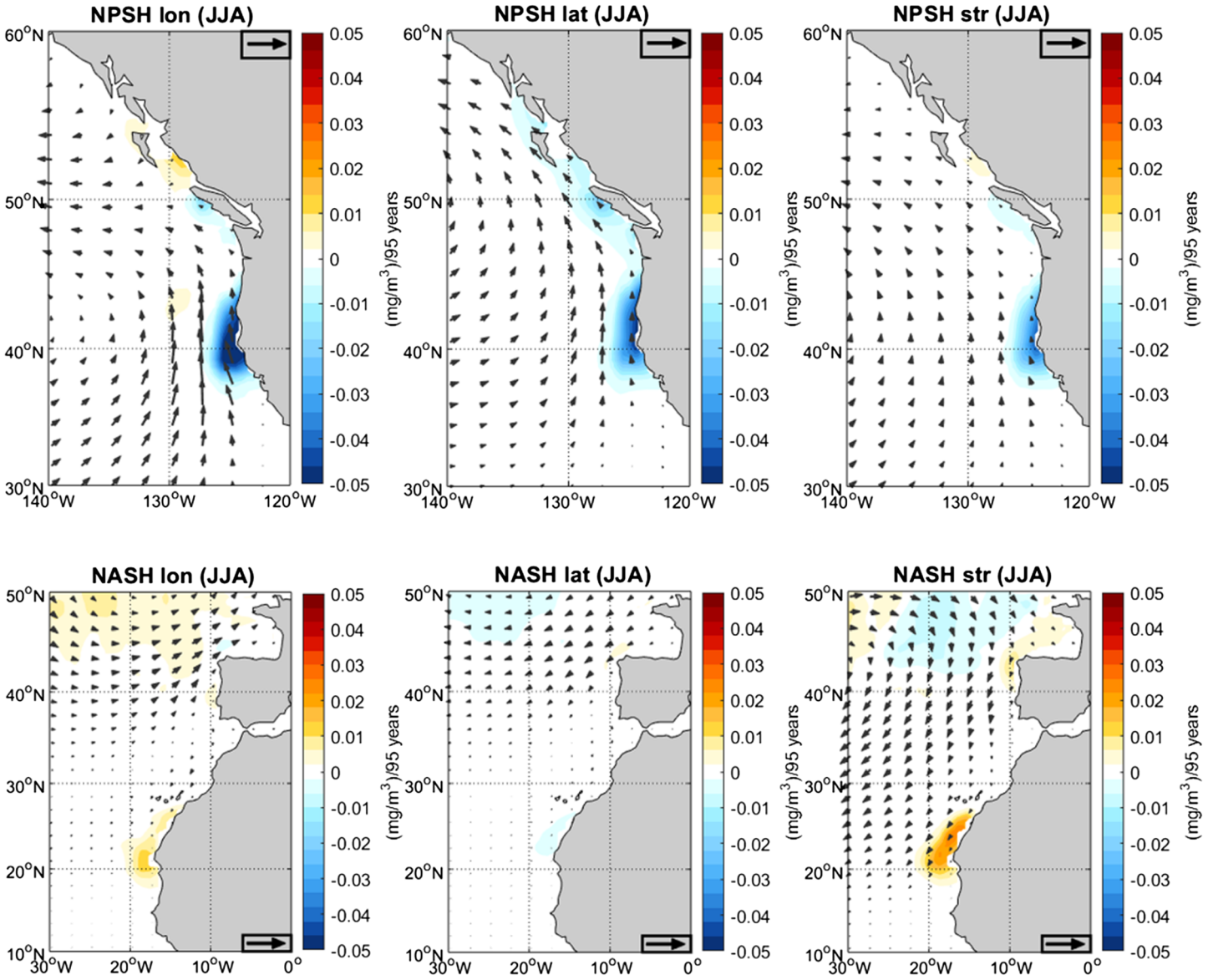

Figure 3. Trends in surface wind stress (arrows) and total chlorophyll (colors) congruent to the NPSH indices (top panels) and NASH indices (bottom panels), for the JJA season only. The bold arrow in the corner represents a wind stress trend of 0.02 N/m^2 per 95 years, for scale. As in Figure 2, chlorophyll is lagged by 1 month in the Pacific only.

We have also repeated the analysis from Figure 2 using observations and reanalysis data (Figure S2). The model and reanalysis wind responses are generally consistent, with one exception: Wind anomalies associated with an eastward shift of the NPSH are northerly in the reanalysis but southerly for the model (Figure 2, top left; see also Figures 1 and 3 of Schmidt & Grise, 2019). We also note that for chlorophyll, the observed time series is not long enough to distinguish statistically significant regression patterns (not shown).

3.2. Trends

The regression patterns in Figure 2 quantify the sensitivity of chlorophyll and wind stress to short-term (month-to-month) variability in the subtropical highs. Ultimately, though, we would like to know whether long-term (centennial-scale) trends in the subtropical highs can drive trends in these upwelling-related variables.

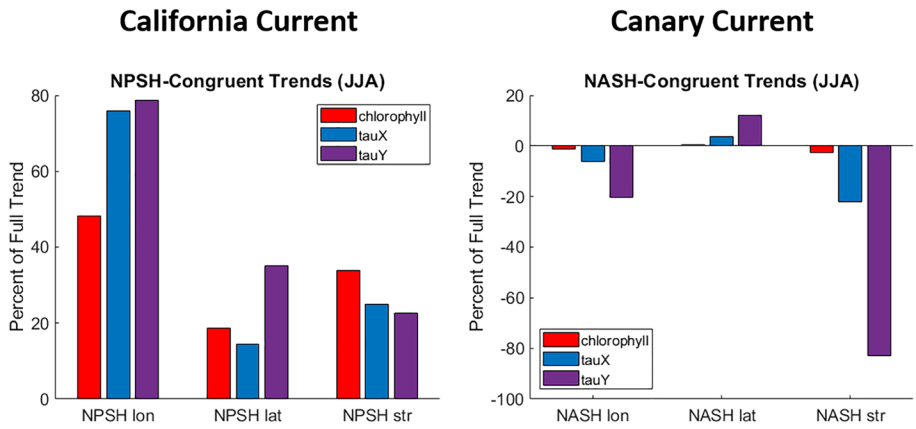

Figure 4. NPSH-congruent (left) and NASH-congruent (right) trends in chlorophyll and the x and y components of surface wind stress (tauX and tauY, respectively)—as in Figure 3—as percentages of the full trends in the same variables. All trends are averaged over the red polygons in Figure 1. As in Figures 2 and 3, chlorophyll is lagged by 1 month in the Pacific only.

To answer this question, we quantify trends associated with individual circulation drivers by using the concept of a "congruent trend." For example, if the regression slope of chlorophyll to NPSH latitude at some location x is $R(x)$, and the trend in NPSH latitude for some model scenario is T, then the trend in chlorophyll congruent to NPSH latitude would be simply $T \cdot R(x)$. This method makes the implicit assumption that the same dynamics by which circulation changes modify eastern boundary currents on month-to-month time scales also operate on the time scales of century-long trends, an assumption we will test in the next section.

During the 21st century (Years 2006–2100 in the RCP 8.5 scenario), CESM projects that the NPSH will shift eastward and slightly southward and weaken, whereas the NASH will shift westward and slightly northward and strengthen. These trends are fairly robust across ensemble members of CESM, but they differ substantially among other CMIP5 models (see Figure 8 of Schmidt & Grise, 2019). Figure 3 shows the trends in CESM-LENS chlorophyll and wind stress congruent with the projected trends in the longitude, latitude, and strength of the subtropical highs. By construction, the spatial patterns are identical to those shown in Figure 2, but they are scaled by the CESM-LENS ensemble-mean trends in the subtropical high indices. Figure 3 (top row) shows that the eastward, southward, and weakening trend in the NPSH are all associated with weakening of upwelling-favorable winds and reduction of chlorophyll. For the North Atlantic, the trends congruent with the trends in NASH longitude and latitude are quite weak, but the projected 21st century strengthening of the NASH is associated with a stronger trend toward more upwelling-favorable wind and more chlorophyll (Figure 3, bottom row).

To put these congruent trends into context, we compare them with the full trends shown in Figure 1 (right column). Figure 4 shows the congruent trends as fractions of the full trend, with both averaged over the red polygons in Figure 1. The modeled trends in the NPSH longitude, latitude, and strength individually account for 48%, 19%, and 34%, respectively, of the full chlorophyll trend in the California Current region and comparable or larger fractions of the surface wind stress trend. In the Canary Current region, by contrast, both the modeled climatological chlorophyll and the modeled full trend in chlorophyll are much larger, and changes in the NASH only account for a very small portion of the full trend—often in the wrong direction (Figure 4, right panel).

As an aside, due to the differences between the observed and model climatology (Figure 1), the actual chlorophyll response to various circulation changes may be stronger and more meridionally elongated than the model-derived results we show here.

3.3. Correlations Across Trends

As mentioned above, one potential weakness of the "congruent trend" method is that it uses short-term sensitivity as a proxy for long-term sensitivity. To test the long-term sensitivity more directly, we wish to determine whether individual ensemble members with larger subtropical high trends also have larger trends in

wind or chlorophyll. We therefore compute the correlation and percent variance explained across the 40 CESM-LENS ensemble members of (for example) the 40 trends in chlorophyll with the 40 trends in NPSH latitude.

For the California Current system, the three NPSH indices and three upwelling-related variables (u and v component wind stress and chlorophyll) give nine correlations. All nine have the same signs that we would expect from Figure 2 (top row), and most are statistically significant, with magnitudes up to about $r = 0.5$ (Table S3). Those relationships with statistically significant correlations each individually explain 7% to 27% of the variance in chlorophyll and wind stress trends in the California Current system.

We can draw two conclusions from this result. First, the model's long-term response to subtropical high shifts is at least qualitatively similar to its short-term response, adding confidence to results derived from the "congruent trend" method. Second, this result shows that a significant fraction (around 7% to 27%) of the uncertainty in upwelling trends can be traced to uncertainty in the future evolution of the NPSH.

3.4. Comparison With the Hadley Cell

The NH Hadley cell has been studied more thoroughly than the subtropical highs, and its future trends are better constrained. Hence, it is worth asking whether the Hadley cell could also explain much of the short-term JJA season variability and trends in upwelling-related variables. It does not. Regressions of wind stress and chlorophyll—as in Figure 2—to short-term variability in Hadley cell width and strength are very weak (not shown). The congruent trends—as in Figure 4—for the Hadley cell are also very small (Figure S3). Finally, the correlations across trends for the Hadley cell and California Current upwelling-related variables are generally weak and not statistically significant (Table S3). We note, however, that the Hadley cell could have more important impacts in other seasons.

4. Conclusions

In this study, we have identified a major driver—and a key source of uncertainty—of trends in the California Current system. The projected 21st century southeastward shift and strengthening of the NPSH each explain large fractions of the projected total trend in wind and chlorophyll off the California coast. Furthermore, comparison across ensemble members of CESM-LENS shows that ensemble members with larger 21st century NPSH shifts also have larger wind and chlorophyll trends. These results extend the findings of previous studies. For example, Rykaczewski et al. (2015) reported a decrease in upwelling-favorable winds in the California Current region in the RCP 8.5 scenario, but here we have been able to more explicitly compute the portions of that full trend in upwelling that can be attributed to various atmospheric circulation features. By contrast with the California Current, projected 21st century trends in the position and strength of the NASH shifts do not explain much of the trend in the Canary Current system, and the NH Hadley cell has little impact on either eastern boundary current system.

We emphasize that due to both model uncertainty and internal variability, the future trends in the subtropical highs themselves are not well constrained (Rykaczewski et al., 2015; Schmidt & Grise, 2019; Shaw & Voigt, 2015; Xiu et al., 2018). Hence, the results found here should not be interpreted as predictions of future upwelling trends. Rather, what we have shown is that much of the uncertainty in the future of California Current upwelling can be traced back to uncertainty in the future evolution of the NPSH.

Data Availability Statement

ERA-Interim data are available at http://apps.ecmwf.int/datasets/data/interim-full-moda, CESM model outputs are available at http://www.cesm.ucar.edu/projects/community-projects/LENS, and observed chlorophyll data are available online (at https://oceancolor.gsfc.nasa.gov/data/10.5067/ORBVIEW-2/SEAWIFS/L3M/CHL/2018/).

Acknowledgments

D. F. S. was supported by the Virginia Space Grant Consortium (Graduate Research Fellowship), D. J. A. was supported by the National Science Foundation (Graduate Fellowship DGE-1144086), and A. J. M. was supported by the National Science Foundation (OCE1600283) and the National Oceanic and Atmospheric Administration (NA17OAR4310106).

References

Amaya, D. J., Siler, N., Xie, S. P., & Miller, A. J. (2018). The interplay of internal and forced modes of Hadley cell expansion: Lessons from the global warming hiatus. *Climate Dynamics*, *51*(1–2), 305–319. https://doi.org/10.1007/s00382-017-3921-5

Bakun, A. (1990). Global climate change and the intensification of coastal upwelling. *Science*, *247*(4939), 198–201. https://doi.org/10.1126/science.247.4939.198

Bakun, A., Black, B. A., Bograd, S. J., García-Reyes, M., Miller, A. J., Rykaczewski, R. R., & Sydeman, W. J. (2015). Anticipated effects of climate change on coastal upwelling ecosystems. *Current Climate Change Reports*, *1*(2), 85–93. https://doi.org/10.1007/s40641-015-0008-4

Belmadani, A., Echevin, V., Codron, F., Takahashi, K., & Junquas, C. (2014). What dynamics drive future wind scenarios for coastal upwelling off Peru and Chile? *Climate Dynamics*, *43*(7–8), 1893–1914. https://doi.org/10.1007/s00382-013-2015-2

Brady, R. X., Alexander, M. A., Rykaczewski, R. R., & Lovenduski, N. S. (2017). Emergent anthropogenic trends in California Current upwelling. *Geophysical Research Letters*, *44*, 5044–5052. https://doi.org/10.1002/2017GL072945

Dee, D. P., Uppala, S. M., Simmons, A. J., Berrisford, P., Poli, P., Kobayashi, S., et al. (2011). The ERA-Interim reanalysis: Configuration and performance of the data assimilation system. *Quarterly Journal of the Royal Meteorological Society*, *137*(656), 553–597. https://doi.org/10.1002/qj.828

ECMWF (2009). ERA Interim reanalysis data, monthly means of daily means. Retrieved from http://apps.ecmwf.int/datasets/data/interim-full-moda

Grise, K. M., Davis, S. M., Simpson, I. R., Waugh, D. W., Fu, Q., Allen, R. J., et al. (2019). Recent tropical expansion: Natural variability or forced response? *Journal of Climate*, *32*(5), 1551–1571. https://doi.org/10.1175/JCLI-D-18-0444.1

He, C., Wu, B., Zou, L., & Zhou, T. (2017). Responses of the summertime subtropical anticyclones to global warming. *Journal of Climate*, *30*, 6465–6479. https://doi.org/10.1175/JCLI-D-16-0529.1

Jacox, M. G., Hazen, E. L., & Bograd, S. J. (2016). Optimal environmental conditions and anomalous ecosystem responses: Constraining bottom-up controls of phytoplankton biomass in the California Current system. *Scientific Reports*, *6*(1), 1–12. https://doi.org/10.1038/srep27612

Kay, J. E., Deser, C., Phillips, A., Mai, A., Hannay, C., Strand, G., et al. (2015). The Community Earth System Model (CESM) large ensemble project: A community resource for studying climate change in the presence of internal climate variability. *Bulletin of the American Meteorological Society*, *96*(8), 1333–1349. https://doi.org/10.1175/BAMS-D-13-00255.1

Levine, X. J., & Boos, W. R. (2019). Sensitivity of subtropical stationary circulations to global warming in climate models: A baroclinic Rossby gyre theory. *Climate Dynamics*, *52*(7-8), 4873–4890. https://doi.org/10.1007/s00382-018-4419-5

Li, L., Li, W., & Kushnir, Y. (2012). Variation of the North Atlantic subtropical high western ridge and its implication to Southeastern US summer precipitation. *Climate Dynamics*, *39*, 1401. https://doi.org/10.1007/s00382-011-1214-y

Li, W., Li, L., Ting, M., & Liu, Y. (2012). Intensification of Northern Hemisphere subtropical highs in a warming climate. *Nature Geoscience*, *5*, 830–834. https://doi.org/10.1038/NGEO1590

Liu, Y., Wu, G., & Ren, R. (2004). Relationship between the subtropical anticyclone and diabatic heating. *Journal of Climate*, *17*, 682–698. https://doi.org/10.1175/1520-0442(2004)017<0682:RBTSAA>2.0.CO;2

Lu, J., Vecchi, G. A., & Reichler, T. (2007). Expansion of the Hadley cell under global warming. *Geophysical Research Letters*, *34*, L06805. https://doi.org/10.1029/2006GL028443

NASA Goddard Space Flight Center, Ocean Ecology Laboratory, Ocean Biology Processing Group (2018). Sea-viewing Wide Field-of-view Sensor (SeaWiFS) chlorophyll data, 2018 reprocessing, NASA OB.DAAC, Greenbelt, MD, USA. https://doi.org/10.5067/ORBVIEW-2/SEAWIFS/L3M/CHL/2018. Accessed on 12/06/2019.

NCAR (2015). CESM large ensemble, monthly-mean. Retrieved from http://www.cesm.ucar.edu/projects/community-projects/LENS

Nigam, S., & Chan, S. C. (2009). On the summertime strengthening of the Northern Hemisphere Pacific sea level pressure anticyclone. *Journal of Climate*, *22*, 1174–1192. https://doi.org/10.1175/2008JCLI2322.1

O'Reilly, J. E., Maritorena, S., Mitchell, B. G., Siegel, D. A., Carder, K. L., Garver, S. A., et al. (1998). Ocean color chlorophyll algorithms for SeaWiFS. *Journal of Geophysical Research*, *103*(C11), 24,937–24,953. https://doi.org/10.1029/98JC02160

Rodwell, M. J., & Hoskins, B. J. (2001). Subtropical anticyclones and summer monsoon. *Journal of Climate*, *14*(15), 3192–3211. https://doi.org/10.1175/1520-0442(2001)014<3192:SAASM>2.0.CO;2

Rykaczewski, R. R., & Dunne, J. P. (2010). Enhanced nutrient supply to the California Current ecosystem with global warming and increased stratification in an earth system model. *Geophysical Research Letters*, *37*, L21606. https://doi.org/10.1029/2010GL045019

Rykaczewski, R. R., Dunne, J. P., Sydeman, W. J., García-Reyes, M., Black, B. A., & Bograd, S. J. (2015). Poleward displacement of coastal upwelling-favorable winds in the ocean's eastern boundary currents through the 21st century. *Geophysical Research Letters*, *42*, 6424–6431. https://doi.org/10.1002/2015GL064694

Schmidt, D. F., & Grise, K. M. (2019). Impacts of subtropical highs on summertime precipitation in North America. *Journal of Geophysical Research: Atmospheres*, *124*, 11,188–11,204. https://doi.org/10.1029/2019JD031282

Seo, H., Brink, K. H., Dorman, C. E., Koracin, D., & Edwards, C. A. (2012). What determines the spatial pattern in summer upwelling trends on the U.S. West Coast? *Journal of Geophysical Research*, *117*, C08012. https://doi.org/10.1029/2012JC008016

Shaw, T., & Voigt, A. (2015). Tug of war on summertime circulation between radiative forcing and sea surface warming. *Nature Geoscience*, *8*, 560–566. https://doi.org/10.1038/ngeo2449

Snyder, M. A., Sloan, L. C., Diffenbaugh, N. S., & Bell, J. L. (2003). Future climate change and upwelling in the California Current. *Geophysical Research Letters*, *30*(15), 1823. https://doi.org/10.1029/2003GL017647

Solomon, A., Polvani, L. M., Waugh, D. W., & Davis, S. M. (2016). Contrasting upper and lower atmospheric metrics of tropical expansion in the Southern Hemisphere. *Geophysical Research Letters*, *43*, 10,496–10,503. https://doi.org/10.1002/2016GL070917

Song, F., Leung, L. R., Lu, J., & Dong, L. (2018). Future changes in seasonality of the North Pacific and North Atlantic subtropical highs. *Geophysical Research Letters*, *45*, 11,959–11,968. https://doi.org/10.1029/2018GL079940

Staten, P. W., Lu, J., Grise, K. M., Davis, S. M., & Birner, T. (2018). Re-examining tropical expansion. *Nature Climate Change*, *8*, 768–775. https://doi.org/10.1038/s41558-018-0246-2

Sydeman, W. J., García-Reyes, M., Schoeman, D. S., Rykaczewski, R. R., Thompson, S. A., Black, B. A., & Bograd, S. J. (2014). Climate change and wind intensification in coastal upwelling ecosystems. *Science*, *345*(6192), 77–80. https://doi.org/10.1126/science.1251635

Taucher, J., & Oschlies, A. (2011). Can we predict the direction of marine primary production change under global warming? *Geophysical Research Letters*, *38*, L02603. https://doi.org/10.1029/2010GL045934

Vallis, G. K., Zurita-Gotor, P., Cairns, C., & Kidston, J. (2015). Response of the large-scale structure of the atmosphere to global warming: Response of atmospheric structure to global warming. *Quarterly Journal of the Royal Meteorological Society*, *141*(690), 1479–1501. https://doi.org/10.1002/qj.2456

Wang, D., Gouhier, T., Menge, B., & Ganguly, A. R. (2015). Intensification and spatial homogenization of coastal upwelling under climate change. *Nature*, *518*(7539), 390–394. https://doi.org/10.1038/nature14235

Waugh, D. W., Grise, K. M., Seviour, W. J., Davis, S. M., Davis, N., Son, S.-W., et al. (2018). Revisiting the relationship among metrics of tropical expansion. *Journal of Climate*, *31*(18), 7565–7581. https://doi.org/10.1175/JCLI-D-18-0108.1

Xiu, P., Chai, F., Curchitser, E. N., & Castruccio, F. S. (2018). Future changes in coastal upwelling ecosystems with global warming: The case of the California Current system. *Scientific Reports*, *8*(1), 1–9. https://doi.org/10.1038/s41598-018-21247-7